

EE

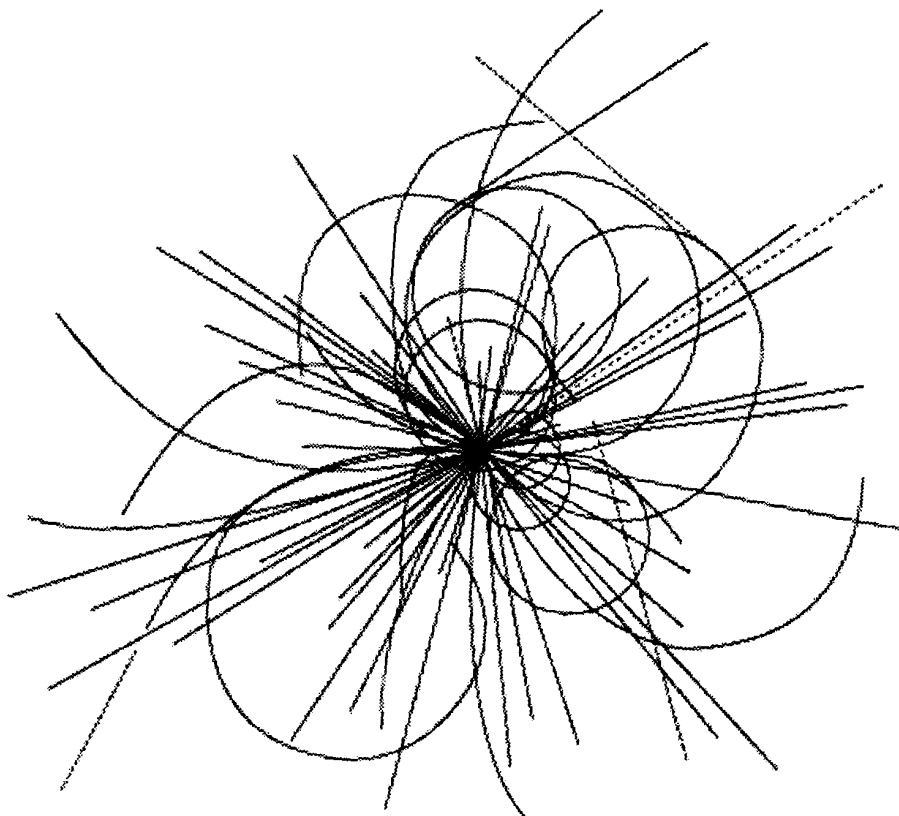
SSCL-Preprint-498 Rev. 1

CERN LIBRARIES, GENEVA



P00023864

Fixed-Structure Suboptimal Feedback Control for Particle Accelerators



Superconducting Super Collider
Laboratory

SSCL Preprint-498 Rev. 1
March 1994

SSCL-Preprint-498 Rev. 1
March 1994
Distribution Category: 414

L.K. Mestha
C. Kwan
K. Yeung

Disclaimer Notice

This report was prepared as an account of work sponsored by an agency of the United States Government. Neither the United States Government or any agency thereof, nor any of their employees, makes any warranty, express or implied, or assumes any legal liability or responsibility for the accuracy, completeness, or usefulness of any information, apparatus, product, or process disclosed, or represents that its use would not infringe privately owned rights. Reference herein to any specific commercial product, process, or service by trade name, trademark, manufacturer, or otherwise, does not necessarily constitute or imply its endorsement, recommendation, or favoring by the United States Government or any agency thereof. The views and opinions of authors expressed herein do not necessarily state or reflect those of the United States Government or any agency thereof.

Superconducting Super Collider Laboratory is an equal opportunity employer.

Fixed-Structure Suboptimal Feedback Control for Particle Accelerators*

L.K. Mestha and C.M. Kwan

Superconducting Super Collider Laboratory[†]
2550 Beckleymeade Ave.
Dallas, TX 75237

K.S. Yeung

The University of Texas at Arlington
Arlington, TX 76019

March 1994

*Submitted to *Particle Accelerators*.

[†]Operated by the Universities Research Association, Inc., for the U.S. Department of Energy under Contract No. DE-AC35-89ER40486.

FIXED-STRUCTURE SUBOPTIMAL FEEDBACK CONTROL FOR PARTICLE ACCELERATORS

L.K. MESTHA AND C.M. KWAN

*Superconducting Super Collider Laboratory**

2550 Beckleymeade Ave.

Dallas, Texas 75237

K.S. YEUNG

University of Texas

Arlington, Texas 76019

ABSTRACT

Application of optimal control theory to optimize the parameters of the low-level rf beam control loops is shown for a low- and a high-intensity circular accelerator. The parameters are: synchronization phase error, beam position error, radial position error, cavity gap voltage error, cavity phase error, cavity tuning error, frequency of the rf system, amplitude of the generator current, phase of the generator current, and tuner bias current. The low-intensity machine is studied by considering the radial, synchronization, and beam phase loops and by ignoring the cavity dynamics. Later we include the cavity model and cover the dynamics of the accelerator system with amplitude, phase, and tuning loops. Flow charts of the computer program are shown to predict and shape the optimal gains starting from the specification on the parameters. The gains are implemented in a particle-tracking code, and with the closed loop system in operation the parameters are tested to be within specification.

* Operated by the Universities Research Association, Inc., for the U.S. Department of Energy under Contract No. DE-AC35-89ER40486.

1 INTRODUCTION

An important problem with low-level rf beam control in fast-cycling circular accelerators is to know the gains in various loops as the beam is accelerated. Most control analyses have been done using the classical approach (based on the single-input single-output method), although the control loops are highly coupled. Fiddling with them by trial and error during the operation of the machine has been the usual practice to improve the performance specifications of parameters. For example, varying the amplitude of the cavity voltage changes the accelerating bucket height, and varying the phase of the rf signal driving the cavity changes the energy received by the beam each time the beam passes through the cavity. Changing the gain in one of the loops—say, the cavity amplitude loop—or adding dynamics to it will invariably change the closed-loop properties of the whole system. In an isolated case, in the presence of only an amplitude loop (with the rest of the loops opened) the effects can be seen on the cavity voltage by looking at the voltage error. Compare this to a typical circular machine, where there are many loops in the low-level rf system that interact with one another in some way. Change in the dynamics of the amplitude loop alone may affect the dynamics of the phase loop. The challenge is: if the dynamics of one loop are changed, can we predict the change required in the other loops so that the parameters are within specification? The answer to this question can be “yes” provided the control system model, including the cavity dynamics, is known and some of the modern feedback control methods are used to predict the gains. Having to know the right gains in each loop is further complicated by the fact that the accelerating parameters are changing with time in a fast-cycling machine. For such complex problems modern optimal control approach is well-suited.

Classical control approach is based on the single-input single-output method, which assumes a highly decoupled system. The modern optimal control theory can deal with the entire coupled system, since the physical system is described by a set of first-order differential equations embedded with control quantities having physical input points. Since most of the

beam and cavity dynamics are used in the model, decoupling of the system is usually not necessary. However, in a typical accelerator, the loop configurations have limitations due to the distributed nature of the cavities. Hence decoupling may still prove useful. Also, the optimal control method is well-suited on occasions where we may need to shape the state and control quantities: the amplitude and phase of the generator currents, cavity detuning functions, frequency and phase shift of the master oscillator, etc.

The optimum control technique, also known as the linear quadratic regulator method, was recently applied to rf systems for circular accelerators at CERN¹ to optimize the injection of a high-intensity beam. The application of the optimum control technique has increased efficiency in industries such as petrochemical, steel, aircraft, and fusion research.² When these techniques are applied to accelerators with proper knowledge of the model, we may get better capture and acceleration efficiencies. Since the optimum control technique is associated with the minimization of a prescribed performance function of the system, we need to formulate a function in terms of the quantities we need to minimize. Suppose we want to minimize the energy in a system where the energy is defined by the sum of the product of the state and a weighting factor, then minimizing the energy corresponds in some sense to keeping the state close to zero. In this paper we define the performance function in terms of the states: synchronization phase error, beam phase error, radial position error, cavity gap voltage error, cavity phase error, and cavity tuning error and control quantities: frequency of the rf system, amplitude of the generator current, phase of the generator current and the tuner bias current. Hence, in our system minimizing the energy leads to minimizing the states as well as the control quantities. We achieve this with feedback with right gains; while doing that, the loop stability is tested.

We first show the application of the optimal control theory to a low-intensity circular machine in which only the global loops (radial, synchronization, and beam phase) are used. We later extend the techniques to include the global loops with the loops around the cavity:

amplitude, phase, and tuning. When the loops around the cavity are included, the system becomes a “fixed structure” because the loop configuration cannot be altered. This is due to the distributed nature of the cavities in a circular machine. The optimum control method assumes that the loop structure can be freely altered. We overcome this restriction by forcing some unwanted gains to zero, then recalculating those needed in the loop. The method is clearly described with a flow chart. The state-space model described in Reference 3 characterizes the low-level rf system. The optimal control techniques shown here can be extended to a more complex system with decoupling filters in some of the loops simply by modifying the state matrices. At the end a computer program will be able to predict the gains required in each loop as we fiddle with any of them. When the gains are implemented, the entire system will be stable, since the stability tests are carried out by taking the physical system into account while predicting optimal gains.

2 LINEAR STATE-SPACE BEAM CONTROL MODEL

A linear model for the beam control loops is derived in Reference 3 for an accelerator with one equivalent cavity system. Let the states be x_1 = synchronization phase error, x_2 = radial position error at high momentum dispersion region, x_3 = beam phase error, x_4 = cavity gap voltage error, x_5 = cavity gap phase error, and x_6 = cavity tuning error, embedded in a column state vector, $x = [x_1, x_2, x_3, \dots, x_6]^T$. Here T is used to define the transpose of a matrix. Also, let the control variables be u_3 = frequency shift, u_4 = generator current amplitude, u_5 = generator current phase, and u_6 = tuning bias regulator current, embedded in a control vector $u = [0, 0, u_3, u_4, \dots, u_6]^T$. If \underline{A} is the system matrix and \underline{B} the input matrix, then the state-space model is given by

$$\begin{aligned}\dot{\underline{x}} &= \underline{A} \underline{x} + \underline{B} \underline{u} + \underline{d} \\ \underline{y} &= \underline{C} \underline{x} .\end{aligned}\tag{1}$$

The output quantity defined by the vector \underline{y} is the product of the output matrix $\underline{C} = \text{diag}\{1, 1, 1, 1, 1, 1\}$ with the state vector \underline{x} . For a fast-cycling accelerator, the disturbance matrix \underline{d} is non-zero, since terms associated with the time rate of change of the cavity gap voltage, synchronous phase, steady-state generator current, and cavity tuning error effect the acceleration process. This matrix is deterministic since it can be compensated by choosing feedforward terms to the control quantities. The exact description of the model is summarized in Table I of Reference 3, which will not be repeated here for simplicity. To limit the complexity, we apply the optimal control theory at first to beam control loops for low-intensity machines, where the cavity low-level rf feedback loops are considered fast compared to global loops and hence are ignored. Later we show the application of this method for a complete low-level rf system.

3 LINEAR OPTIMAL CONTROL FOR LOW-INTENSITY OPERATION

Here, when the radial loop, beam phase loop, and synchronization loops are connected to a common summing point as in Figure 1, the conventional optimal control techniques outlined in Appendix A are used to optimize the gains (see Table I for a state-space model of the low-intensity machine). For low-intensity machines, if we follow the loop configuration of Figure 1, then the system structure has a dimension of three with the feedback control vector $\underline{u} = [0, 0, u_3]^T$, defined by $\underline{u} = -\underline{k}\underline{x}$, where the state matrix is $\underline{x} = [x_1, x_2, x_3]^T$, and the gain matrix is \underline{k} given by

$$\underline{k} = \begin{bmatrix} 0 & 0 & 0 \\ 0 & 0 & 0 \\ k_1 & k_2 & k_3 \end{bmatrix}. \quad (2)$$

The loop gains k_1 , k_2 , and k_3 are specified for synchronization, radial, and beam phase loops, respectively. Our specified objective is to calculate the values for k_1 , k_2 , and k_3 so that the system is driven along a three-dimensional optimal state trajectory such that a predefined performance function is minimized. We will follow the exact procedure described in

Appendix A and show how k_1 , k_2 , and k_3 can be evaluated at each point in the accelerating cycle.

3.1 Performance Function

In theory, there is no unique way of defining a performance function for a specific control problem with system dynamics described by state equations. We will formulate the trial performance function, J , with emphasis on the maximum control quantities and the maximum allowable deviations in states. To control the beam we would require the states x_1 , x_2 , and x_3 to be maintained to within specific maximum values at a given time in the cycle. To achieve the specification on the state variables, we have a limited allowable deviation in the control variable u_3 , in Hz with the acceleration cycle time. Based on these constraints let us choose a performance function to weigh the state and control variables as follows:

$$J = \frac{1}{2} \int_{t_0}^{T_f} (\underline{x}^T \underline{Q} \underline{x} + \underline{u}^T \underline{R} \underline{u}) dt , \quad (3)$$

where the weighting matrices \underline{Q} and \underline{R} are defined in Eqs. (A.2) and (A.3), respectively, and t_0 and T_f are the initial and final time of the control process. Thus we have specified weights in \underline{Q} for the controlled parameters (states) and weights in \underline{R} for the frequency shift. Selection of these weights determines the time response of the overall control system. As we mentioned earlier, the quadratic form shown in Eq. (3) is not the only way, since it has the intuitive resemblance to least-squares: it corresponds in some sense to energy in the control system. In optimal control, since we are required to minimize J , which is constrained by the linear system dynamics as described by Eq. (1), a Hamiltonian system is constructed. By solving the Hamiltonian system, two important equations are derived: the optimal control, $\underline{u} = \underline{u}^{opt}$, in terms of \underline{R} , \underline{B} , \underline{x} matrices, and a function, \underline{S} matrix, which is a solution of the differential matrix Riccati equation as shown below:

$$\underline{u}^{opt} = -\underline{R}^{-1}\underline{B}^T\underline{S}\underline{x} = -\underline{k}^{opt}\underline{x} \quad (4)$$

$$-\dot{\underline{S}} = \underline{A}^T\underline{S} + \underline{S}\underline{A} - \underline{S}\underline{B}\underline{R}^{-1}\underline{B}^T\underline{S} + \underline{Q} . \quad (5)$$

The new time-varying gain matrix \underline{k}^{opt} represents the optimal feedback gains:

$$\underline{k}^{opt} = \underline{R}^{-1}\underline{B}^T\underline{S} . \quad (6)$$

Hence the optimal state trajectories are determined by substituting Eq. (4) in system Eq. (1) and using numerical methods to solve for $\underline{x}(t)$. In the case where $T_f \rightarrow \infty$ in Eq. (3), \underline{k}^{opt} is a constant matrix. Then the optimal trajectory is given by

$$\underline{x}^{opt} = \exp\left(\left(\underline{A} - \underline{B}\underline{k}^{opt}\right)t\right)\underline{x}_0 , \quad (7)$$

where \underline{x}_0 are the initial values of the states at injection. Eq. (7) must be used when the parameters in matrices \underline{A} and \underline{B} are not time-varying. We describe below the essential steps involved in evaluating the optimal gains and the optimal states.

3.2 Evaluation of Optimal Gain

The optimal gain vector, \underline{k}^{opt} , is solved by solving for the steady-state value of the differential matrix Riccati Eq. (5) for $q_1 = 1$, $q_2 = 1$, and $q_3 = 1$ for \underline{Q} , and $r_1 = 1$, $r_2 = 1$, and $r_3 = 1$ for \underline{R} at $t = 0$ in the acceleration cycle, and then substituting the results in Eq. (6). The steady-state value of matrix \underline{S} is obtained from the procedure described in Appendix A. The optimal gain matrix is substituted in Eq. (7) to solve for the optimal values of the states \underline{x}^{opt} . Now compare the calculated optimal states with the specifications for the states. If the values are greater than specified values, then change the scalar multipliers in the \underline{Q} and \underline{R} matrices in Eqs. (A.2) and (A.3) to higher than 1, and then solve for the optimal gain and optimal states. Compare the optimal states to the specified values again. If the states are still not acceptable, repeat the entire process for a new set of scalar multipliers. According to optimal

control theory (see how to select \underline{Q} and \underline{R} matrices in Anderson, Reference 4), by multiplying all the elements of \underline{Q} and \underline{R} by a larger and larger value, the state vectors will converge to a specified value. During the iterations we have kept the matrices \underline{A} and \underline{B} unchanged; these were computed once at $t = 0$ in the acceleration cycle. After we reach a compromise on the optimal quantities of the states and control vector, we can then go to a second time interval, $t = 2$ ms (or any other subintervals in the acceleration cycle), and compute optimal gains with a new set of values in \underline{A} and \underline{B} matrices. For each value of $t = 0, t = 1$ ms, ..., 50 ms, tabulate the optimal gain matrix. In this way we can calculate the time-varying gains during the entire acceleration cycle. In control literature this approach is also known as “gain scheduling” and is successfully applied in the aerospace industry. In Figure 2 a flow chart of the iteration steps is shown. Figure 3 shows the optimal gain profile with time. Figure 4 is plotted to show the state trajectories x_1 , x_2 , and x_3 when computed using Eq. (7) and the particle-tracking code. Figure 5 is shown to compare the control, \underline{u}^{opt} , when computed using Eq. (7) and the particle-tracking code. The dashed lines are not smooth since the time-varying gains have steps at 1 ms. However, while implementing the gains they can be computed at a much finer time interval.

4 FIXED-STRUCTURE OPTIMAL FEEDBACK (HIGH-INTENSITY CASE)

To illustrate the application of linear optimal control for machines with beam loading problems, we must consider the cavity dynamics and associated loops surrounding the cavity. When the cavity loops are considered, it becomes almost impossible to apply those techniques mentioned in Appendix A without considerable modifications. This is because it is normal practice with proton accelerators to have more than one accelerating cavity system, with each system having amplitude, phase, and tuning loops local to the cavities arranged to reduce beam loading transients on the gap voltage. The amplitude and phase control is done by modulating the phase and amplitude of the generator currents with fast phase and amplitude loops. The tuning is usually controlled by changing the bias current, which has inherent limitations on the

bandwidth due to slow tuners. These loops affect the amplitude and phase of the cavity gap voltage of each cavity as compared to the global beam control loops, since the global loops change the amplitude and phase of the voltage of the entire rf system together with respect to the beam. Hence, if we change the amplitude of the global rf signal alone, then the effective sum of all the cavity voltage changes, provided there are no local amplitude loops on each cavity. In other words, we cannot control the voltage on an individual cavity by amplitude-modulating the rf signal global to the ring accelerating system. By this we mean that although the individual cavity loops can be brought to one point to control all the states, the control will not be so effective. While applying optimal control techniques, we may need to do this depending on the solution of the optimal gain matrix, \underline{k}^{opt} , because of unwanted elements in the gain matrix resulting from the solution of the non-linear Riccati equation. The argument will be more clear when we look at the optimal solution by first defining the control strategy as below.

Let the control vector for the loops shown in Figure 1 be defined in terms of feedback gains and the state vector as follows:

$$\begin{bmatrix} 0 \\ 0 \\ u_3 \\ u_4 \\ u_5 \\ u_6 \end{bmatrix} = - \begin{bmatrix} 0 & 0 & 0 & 0 & 0 & 0 \\ 0 & 0 & 0 & 0 & 0 & 0 \\ k_1 & k_2 & k_3 & 0 & 0 & 0 \\ 0 & 0 & 0 & k_4 & 0 & 0 \\ 0 & 0 & 0 & 0 & k_5 & 0 \\ 0 & 0 & 0 & 0 & 0 & k_6 \end{bmatrix} \begin{bmatrix} x_1 \\ x_2 \\ x_3 \\ x_4 \\ x_5 \\ x_6 \end{bmatrix} . \quad (8)$$

The gain elements k_1, k_2, k_3 correspond to global loops, and elements k_4, k_5, k_6 correspond to local loops for an equivalent cavity system. The placement of these gains in Eq. (8) is based on the loop configuration shown in Figure 1. In vector form Eq. (8) can be written as:

$$\underline{u} = - \underline{k} \underline{x} . \quad (9)$$

Many elements of the gain matrix, \underline{k} , are set equal to zero to arrange the loop configuration to the form shown in Figure 1. If we compute the optimal gain matrix, \underline{k}^{opt} , by solving the Riccati equation using the method described in Appendix A, then the optimal gain matrix may come out with more than six non-zero elements, k_1, k_2, \dots, k_6 , shown in Eq. (8). For example, if the element in the 4th row and 3rd column is non-zero, (k_{43}), with a magnitude comparable to element k_4 , then the control u_4 will be in the form $u_4 = -(k_{43}x_3 + k_4x_4)$. This means the amplitude of the generator current of one of the power amplifiers has to be modulated with the inputs from two states—namely, the beam phase error (x_3) and the amplitude error (x_4). It is as good as adding another loop on top of all the loops described in Figure 1. Thus the structure of the control loops is changed. To alleviate this problem, i.e., to fix the loop structure unchanged, we force the unwanted non-zero gain elements, such as k_{43} , from the optimal gain matrix to zero and then test for the stability of the loops. If the system is still stable we then recalculate the new optimal gains by solving the Riccati equation with the new set of forced gain matrices. In order to do this we need the Riccati Eq. (5) in terms of the gain matrix, \underline{k} . This can be done as follows. Rearranging Riccati Eq. (5) in terms of the optimal gain matrix we get:

$$-\dot{\underline{S}} = \underline{A}^T \underline{S} - (\underline{B} \underline{k}^{opt})^T \underline{S} + (\underline{B} \underline{k}^{opt})^T \underline{S} + \underline{S} \underline{A} - \underline{S} \underline{B} \underline{k}^{opt} + \underline{S} \underline{B} \underline{k}^{opt} - \underline{S} \underline{B} \underline{R}^{-1} \underline{R} \underline{R}^{-1} \underline{B}^T \underline{S} + \underline{Q}.$$

By making use of Eq. (6) and the following known relationship:

$$(\underline{B} \underline{k}^{opt})^T \underline{S} = \underline{S} \underline{B} \underline{k}^{opt} = (\underline{k}^{opt})^T \underline{R} \underline{k}^{opt}$$

we get the new Riccati equation in terms of the optimal gain matrix \underline{k}^{opt} and system matrix \underline{A} :

$$-\dot{\underline{S}} = (\underline{A} - \underline{B} \underline{k}^{opt})^T \underline{S} + \underline{S} (\underline{A} - \underline{B} \underline{k}^{opt}) + (\underline{k}^{opt})^T \underline{R} \underline{k}^{opt} + \underline{Q}. \quad (10)$$

We use Eq. (10) in place of Eq. (5) to compute the optimal gains for the fixed-structure loop configuration. As we said earlier, the fixed structure is due to the way the global loops are integrated with more than one cavity system. Otherwise, in the implementation of optimal control, if there is only one cavity we can compute the gains using conventional techniques (shown in Appendix A) even for heavy beam loading cases.

While computing the optimal gain matrix, \underline{k}^{opt} , by forcing the unwanted gain elements to zero, we need to monitor the way the performance function, J , is behaving. In order to do this, we have to define the performance function in terms of the optimal gain matrix. This is done by substituting the time domain state Eq. (7) and the optimal control matrix $\underline{u}^{opt} = -\underline{k}^{opt}\underline{x}^{opt}$ in Eq. (3), and then simplifying:

$$J = \frac{1}{2} \int_{t_0}^T \underline{x}_0^T \left\{ \left[e^{-(\underline{A} - \underline{B}\underline{k}^{opt})t} \right]^T \left[\underline{Q} + (\underline{k}^{opt})^T \underline{R} \underline{k}^{opt} \right] \left[e^{-(\underline{A} - \underline{B}\underline{k}^{opt})t} \right] \right\} \underline{x}_0 dt . \quad (11)$$

Overall computations involve several iterations, because for each set of forced gain matrices we need to observe the stability bounds and the way the performance function is behaving to reach a convergent optimal solution. Section 5 outlines the individual steps to determine the optimal solution.

5 DESCRIPTION OF THE METHOD

Figure 6 is a flow chart of the computational steps outlined below:

Step 1: Calculate matrices \underline{A} and \underline{B} from the machine parameters at, say, $T = 1$ ms, using the model summarized in Table I of Reference 3.

Step 2: Assume some initial estimated gain values for $k_1, k_2, k_3, \dots, k_6$ in the gain matrix in Eq. (8) so that the closed loop characteristic matrix, $\underline{A} - \underline{B}\underline{k}$, is asymptotically stable. At this stage the stability can be checked by calculating the eigen values of the matrix, $\underline{A} - \underline{B}\underline{k}$, and then observing whether all the eigen values lie in the left half of the s -plane.

Step 3: Assume the \underline{Q} and \underline{R} matrix as follows:

$$\underline{Q} = \begin{bmatrix} \frac{q_1}{(x_1)_m^2} & & & & & \\ & \frac{q_2}{(x_2)_m^2} & & & & \\ & & \circ & & & \\ & & & \ddots & & \\ & & & & \circ & \\ & & & & & \frac{q_6}{(x_6)_m^2} \end{bmatrix} \quad \underline{R} = \begin{bmatrix} \frac{r_1}{(u_1)_m^2} & & & & & \\ & \frac{r_2}{(u_2)_m^2} & & & & \\ & & \circ & & & \\ & & & \ddots & & \\ & & & & \circ & \\ & & & & & \frac{r_6}{(u_6)_m^2} \end{bmatrix} \quad (12)$$

Step 4: Calculate the performance function, J , using Eq. (11).

Step 5: Solve the Riccati differential matrix equation shown in Eq. (10). Use the steady-state value to determine the optimal gain matrix, \underline{k}^{opt} , using Eq. (6).

Step 6: If some of the elements other than $k_1, k_2, k_3, \dots, k_6$ in the gain matrix, \underline{k}^{opt} , are non-zero, then force them to be equal to zero. This is the constraint we have imposed on the gain matrix in order to retain the structure of the overall feedback system.

Step 7: Check for stability by looking at the eigen values of the characteristic equation, $\underline{A} - \underline{B} \underline{k}^{opt}$, using the forced gain matrix. If it is asymptotically stable, then compute the value of J by using Eq. (11) with the gain matrix as \underline{k}^{opt} . Otherwise, change the gain matrix and go to Step 2. After obtaining J , compare the new value of J with that calculated in the previous iteration of this step. If the new value of J is lower than the previous value, then we are progressing toward an optimal solution. Then, repeat Steps 5 to 7 until the performance function J no longer differs from the previous iteration. In Figure 7 the normalized value of J is plotted at 1 ms for 20 iterations. It has converged to a steady value within 10 iterations. At this time in the iteration the performance function is minimal, and hence the forced gain matrix yields optimal state trajectories. The local minimum after 4 iterations is only the transient in J

before reaching steady state. The forced gain matrix at local minima does not correspond to optimum solution.

Step 8: Calculate the optimal state trajectories and control quantities using Eqs. (7) and (8), respectively, by using the forced optimal gain matrix obtained in Step 7. If the states and control quantities are not within the specifications, then change the weighting elements such as q_1, q_2, \dots, q_6 and r_1, r_2, \dots, r_6 on appropriate elements of the weighting matrices \underline{Q} and \underline{R} in Step 3. Then follow Steps 4 to 8 until the states and control quantities are within the specifications.

The process is continued through the whole acceleration cycle by increasing the time step in increments of 1 ms, 2 ms, 3 ms, and so on. In this way we can compute the optimal gain values so that the state trajectories are within the specifications in spite of the fixed loop structure. Figure 8 shows the time-varying optimal gains in all the loops; Figures 8(a–c) are the time-varying gains in the global loops when computed by including the cavity dynamics, which compares well with those shown in Figure 3. The optimal state trajectories and the control quantities are shown in Figures 9 and 10, respectively, for a short duration at the beginning of the acceleration cycle. The dashed lines are those obtained using the particle-tracking code that includes the cavity dynamics.⁵ The solid lines are the optimum trajectories obtained by numerically integrating the linear state-space model. Both the solid lines and the dashed lines use the same optimal gains in the feedback loops. As we see from the plots, the transients do not compare very well due to the non-linearities we have ignored in the linear state-space model compared to the tracking code. A better comparison could be made in a real machine when it becomes available. Then we could see whether the optimal states can be predicted by merely solving the linear state-space model. Clearly, there is an advantage if the optimal state trajectories compare very well with the real-world situation, since the control system time response can be shaped with off-line simulation iteratively by changing the weighting factors in the optimal function, J . The simulations will be close to the predicted

optimal trajectories if the model we have used is accurate. On the whole, our predictions of the settling time of the transients are good. Also, the transients are predicted well some time after injection.

While designing the optimal gains, constraints may need to be introduced on some of the loop gains, depending on the practical limits of the rf system. Off-line gain shaping is helpful to get *a priori* information on the possible consequences on the beam if the same gains were to be used on the machine. Effectively, this approach boils down to investigating the control effects on the computer first before trying on the real machine, rather than choosing to follow the classical trial-and-error approach of the past with lots of beam study time. At the end, both methods may very well give the same results! Also the effects of external disturbances and the model variations on the optimal trajectories is not covered in this paper although such an analysis is essential to justify the robustness of the control system. The emphasis as a first step, was largely to show a new approach to rf feedback system design using well established modern control theory. For a complete design, fine tuning of the gains can be done with some knowledge of noise and other uncertainties when the basic approach works on a real machine.

6 CONCLUSIONS

The linear optimal control method is applied to a fast-cycling circular accelerator such as the Superconducting Super Collider Low Energy Booster. The predicted optimal state trajectories are compared with the particle-tracking code for a low beam intensity case (without the cavity model) and for a high beam intensity case (with the cavity model). Once the system model is known, the application of optimal control to the low beam intensity case is straightforward. But several alterations were required in the algorithm to consider loops around the cavity, since the distributed nature of the cavities in a circular machine does not allow flexibility to change the structure of the loops.

The optimal control technique may become well-suited for calculating the gains to meet the specifications on different state variables in the presence of external disturbances and other

uncertainties. At this stage, the extent to which the optimal gains will help in optimizing the capture and acceleration efficiencies is unknown. There is, however, some indication in our limited simulation studies that the time-varying gains tend to give reduced beam phase oscillations. Since the approach is based on the total system description that includes accurate models of the cavity and beam dynamics, it may very well increase the capture, acceleration, and extraction efficiencies. The optimal part may not be that critical, but the ability of the control to deal with the entire multi-input, multi-output coupled system rather than the decoupled classical design practices may be of overall benefit to the accelerator operation. Furthermore, the ability of the optimal control to guarantee stability of the entire low-level rf system and still allow the flexibility to shape the gains and the control quantities may take precedence over the complexity of the technique.

APPENDIX A

A.1 OPTIMAL FEEDBACK CONTROL

In generating an optimal control, a function representing the ultimate system performance must first be created. For example, in the low beam intensity case, the objective of the optimal control is to find the right frequency shift, \underline{u} , to keep the states x_1 , x_2 , and x_3 under specified limits (or to reach zero), and while doing so to keep the frequency shift, \underline{u} , (quantifying control energy), to a value as low as possible. Under no circumstances is the system permitted to go unstable. One such performance function can be assumed in the following form:

$$J = \frac{1}{2} \int_{t_0}^{T_f} (\underline{x}^T \underline{Q} \underline{x} + \underline{u}^T \underline{R} \underline{u}) dt , \quad (\text{A.1})$$

where \underline{Q} and \underline{R} are symmetric and positive definite matrices, \underline{x}^T and \underline{u}^T are the transposed matrices of the state and control quantities, and t_0 and T_f are the initial and final times in the

integral equation for the cost. The weighting matrices are defined as follows:

$$\underline{Q} = \text{diag}\{q_i/(x_i)_m^2\} \quad i = 1, 2, \dots, 6 \quad (\text{A.2})$$

$$\underline{R} = \text{diag}\{r_i/(u_i)_m^2\} \quad i = 1, 2, \dots, 6, \quad (\text{A.3})$$

where $(x_i)_m, i = 1, 2, \dots, 6$, are the specified maximum values of the states and $(u_i)_m, i = 1, 2, \dots, 6$, are the maximum values of the control variable. Arranging the elements inside the weighting matrices is purely optional and depends on final performance objectives. There is, however, no scientific method available to select an optimal performance function for a given system.

After having defined the performance function and \underline{Q} and \underline{R} matrices, the optimal control problem is to find the control vector $\underline{u} = \underline{u}^{opt}$ such that when the control vector is applied to the system, it drives the system states described by the state Eq. (1) along a trajectory $\underline{x} = \underline{x}^{opt}$ such that the performance function, J , over a specified time is minimal. One of the straightforward ways to minimize the performance function is to create a Hamiltonian:

$$H = \frac{1}{2}(\underline{x}^T \underline{Q} \underline{x} + \underline{u}^T \underline{R} \underline{u}) + \underline{\lambda}^T (\underline{A} \underline{x} + \underline{B} \underline{u}) . \quad (\text{A.4})$$

The new function $\underline{\lambda}^T$ is the transpose of the vector containing elements known as Lagrange Multipliers. This is an intermediate vector used in the derivation of optimal control, \underline{u}^{opt} . We do not need to compute it. The necessary condition for J to be minimal is derived from a Taylor series expansion,⁶ which is given by

$$\frac{\partial H}{\partial \underline{x}} = - \dot{\underline{\lambda}} = \underline{Q} \underline{x} + \underline{A}^T \underline{\lambda} \quad (\text{A.5})$$

$$\frac{\partial H}{\partial \underline{u}} = 0 = \underline{R} \underline{u} + \underline{B}^T \underline{\lambda} \quad (\text{A.6})$$

$$\frac{\partial H}{\partial \underline{\lambda}} = \dot{\underline{x}} = \underline{A} \underline{x} + \underline{B} \underline{u} . \quad (\text{A.7})$$

From Eq. (A.6) the optimal control in terms of Lagrange Multipliers is written as follows:

$$\underline{u}(t) = -\underline{R}^{-1}\underline{B}^T\underline{\lambda} . \quad (\text{A.8})$$

Furthermore, we substitute Eq. (A.8) into Eq. (A.7) and rewrite the resulting equation and Eq. (A.5) to get the following Hamiltonian system equation:

$$\begin{bmatrix} \dot{\underline{x}} \\ \dot{\underline{\lambda}} \end{bmatrix} = \begin{bmatrix} \underline{A} & -\underline{B}\underline{R}^{-1}\underline{B}^T \\ -\underline{Q} & -\underline{A}^T \end{bmatrix} \begin{bmatrix} \underline{x} \\ \underline{\lambda} \end{bmatrix} . \quad (\text{A.9})$$

This Hamiltonian system equation has a solution for $\underline{\lambda}$ that can be assumed as

$$\underline{\lambda} = \underline{S}\underline{x} . \quad (\text{A.10})$$

Substituting Eq. (A.10) into Eq. (A.9), we obtain

$$-\dot{\underline{S}} = \underline{A}^T\underline{S} + \underline{S}\underline{A} - \underline{S}\underline{B}\underline{R}^{-1}\underline{B}^T\underline{S} + \underline{Q} . \quad (\text{A.11})$$

This is a Riccati equation, and $\underline{S}(t)$ will be its solution. Thus, if we can solve the Riccati equation, then the optimal control is given by

$$\underline{u}^{opt} = -\underline{R}^{-1}\underline{B}^T\underline{S}\underline{x} = -\underline{k}^{opt}\underline{x} , \quad (\text{A.12})$$

where the feedback gain matrix \underline{k}^{opt} is given by

$$\underline{k}^{opt} = \underline{R}^{-1}\underline{B}^T\underline{S} . \quad (\text{A.13})$$

The optimal gain is determined by solving the Riccati Eq. (A.11) backward in time for $\underline{S}(t)$ off-line, since the states are not required in Eq. (A.11). Optimal performance function is obtained by substituting Eq. (A.12) into Eq. (A.1), which is given by

$$J^{opt} = \frac{1}{2} \underline{x}^T \underline{S}(t) \underline{x} . \quad (\text{A.14})$$

A.2 SOLUTION OF RICCATI EQUATION

The Riccati equation must be iterated backward in time since final conditions are known than the initial.⁶ Since most Runge-Kutta routines work forward in time, we can use the following method to integrate Eq. (A.11) by changing the time variable, t , to a new variable τ , which is

$$\tau = T_f - t . \quad (\text{A.15})$$

Then by differentiating Eq. (A.15) with respect to time, t , and then substituting for $dt = -d\tau$ in Eq. (A.11), we obtain the following Riccati equation:

$$\dot{\underline{S}}_b = \underline{A}^T \underline{S}_b + \underline{S}_b \underline{A} - \underline{S}_b \underline{B} \underline{R}^{-1} \underline{B}^T \underline{S}_b + \underline{Q} \quad (\text{A.16})$$

$$\underline{S}(t) = \underline{S}_b(T_f - t) . \quad (\text{A.17})$$

To solve the Riccati equation, integrate Eq. (A.16) forward in time from $t = 0$ to $t = T_f$ and then reverse the results to obtain $\underline{S}(t)$, as in Eq. (A.17). For example, in the case of the Low Energy Booster, while solving Riccati equation, (A.16), $t = 0$ corresponds to 50 ms and $t = T_f$ corresponds to 0 ms. Thus, the parameters \underline{A} , \underline{B} , \underline{R} and \underline{Q} have to be selected starting from 50 ms down to 0 ms as we integrate Eq. (A.16) forward in time from $t = 0$ to $t = T_f$. The initial value $\underline{S}_b(0)$ is obtained by solving Eq. (A.16) under steady state for $\dot{\underline{S}}_b(0)$ and \underline{A} , \underline{B} , \underline{R} and \underline{Q} at 50 ms. For the parameters of the LEB we found that only the steady-state solution of $\underline{S}(t)$ was sufficient in calculating the optimal gain. In Table A.I the computational sequence is summarized. The gain $\underline{k}^{opt}(t)$ is computed for known values of \underline{A} , \underline{B} , \underline{Q} , and \underline{R} matrices at a given time in the accelerating cycle, each time by using the steady-state solution of $\underline{S}(t)$.

A.3 OVERALL LOOP STABILITY

If the system is stabilizable⁷ and if we select \underline{Q} so that $(\underline{A}, \sqrt{\underline{Q}})$ is observable,⁷ then the feedback gain $\underline{k}^{opt} = \underline{k}^{opt}(\infty) = \underline{R}^{-1}\underline{B}^T\underline{S}(\infty)$ results in a stable closed-loop plant. Here, $\underline{S}(\infty)$ is a limiting solution of the Riccati equation. This statement is proved in Theorem 3.4-2 of Reference 6. The limiting solution is nothing but the steady-state value of $\underline{S}(t)$ obtained by solving Eq. (A.11). For the Low Energy Booster we can never have the true optimal gains in practice, since the parameters will have changed before we have found a limiting solution of the Riccati equation. However, the feedback gains represented by $\underline{k}^{opt}(t)$ give conditions close to the optimal situation. Hence this type of optimal control is also known as “suboptimal control.” With these gains to keep the overall system stable, we have to carefully choose the weighting matrix \underline{Q} so that $(\underline{A}, \sqrt{\underline{Q}})$ is observable.

TABLE I. Linear state-space beam control model for low-intensity machine.

$$\begin{bmatrix} \dot{x}_1 \\ \dot{x}_2 \\ \dot{x}_3 \end{bmatrix} = \begin{bmatrix} a_{11} & a_{12} & 0 \\ 0 & a_{22} & a_{23} \\ 0 & a_{32} & 0 \end{bmatrix} \begin{bmatrix} x_1 \\ x_2 \\ x_3 \end{bmatrix} + \begin{bmatrix} 0 & 0 & 0 \\ 0 & 0 & 0 \\ 0 & 0 & b_{31} \end{bmatrix} \begin{bmatrix} 0 \\ 0 \\ u_3 \end{bmatrix}$$

$\dot{\underline{x}} = \underline{A} \underline{x} + \underline{B} u$
 v^s velocity of a synchronous particle
 γ_T transition gamma
 η^s slip factor
 f^s rf frequency
 R^s ideal radius
 β^s v^s/c
 c speed of light
 E^s Energy of particle
 $a_{11} = \frac{\dot{v}^s}{v^s}$ $A_1 = \frac{(\beta^s)^2 \gamma_T^2 E^s}{R^s}$
 $a_{12} = -\frac{v^s \eta^s \gamma_T^2}{R^s}$ $a_{32} = \frac{2\pi f^s \eta^s \gamma_T^2}{R^s}$
 $a_{22} = -\frac{\dot{A}_1}{A_1}$ $b_{31} = 2\pi$
 $x_1 = \delta S$ $x_3 = \delta \phi^s$
 $x_2 = \delta R$ $u = \delta f^c$

TABLE A.I. Closed-loop optimal control.

Riccati Equation:	$\dot{\underline{S}}_b = \underline{A}^T \underline{S}_b + \underline{S}_b \underline{A} - \underline{S}_b \underline{B} \underline{R}^{-1} \underline{B}^T \underline{S}_b + \underline{Q}$ $\underline{S}(t) = \underline{S}_b(T_f - t)$
Optimal Gains:	$\underline{k}^{opt} = \underline{R}^{-1} \underline{B}^T \underline{S}$
Optimal States:	$\underline{x}^{opt} = \exp\left((\underline{A} - \underline{B} \underline{k}^{opt}) t \right) \underline{x}_0$
Optimal Control:	$\underline{u}^{opt}(t) = - \underline{k}^{opt}(t) \underline{x}$
Optimal Performance Function:	$J^{opt}(t) = \frac{1}{2} \underline{x}^T(t) \underline{S}(t) \underline{x}(t)$

FIGURE CAPTIONS

- FIGURE 1 Schematic loop diagram of low-level rf beam control loops for the SSC Low Energy Booster.
- FIGURE 2 Flow chart for calculating the optimal gains for low-intensity machines.
- FIGURE 3(a) Gain in synchronization loop with time.
- FIGURE 3(b) Gain in radial loop with time.
- FIGURE 3(c) Gain in beam phase loop with time.
- FIGURE 4(a) Variation of synchronization phase error with time.
- FIGURE 4(b) Variation of radial position error with time.
- FIGURE 4(c) Variation of beam phase error with time.
- FIGURE 5 Variation of control (frequency shift) with time.
- FIGURE 6 Flow chart to evaluate optimal gains for high-intensity machines.
- FIGURE 7 Normalized optimal function, J , at 1 ms.
- FIGURE 8(a) Gain in synchronization loop with time.
- FIGURE 8(b) Gain in radial loop with time.
- FIGURE 8(c) Gain in beam phase loop with time.
- FIGURE 8(d) Gain in amplitude loop with time.
- FIGURE 8(e) Gain in cavity phase loop with time.
- FIGURE 8(f) Gain in cavity tuning loop with time.
- FIGURE 9(a) Variation of synchronization phase error with time.
- FIGURE 9(b) Transients in radial position error.
- FIGURE 9(c) Transients in beam phase error.
- FIGURE 9(d) Transients in amplitude error.
- FIGURE 9(e) Transients in cavity voltage phase error.

FIGURE 10(a) Transients in frequency control.

FIGURE 10(b) Transients in the amplitude of the generator current.

FIGURE 10(c) Transients in the phase of the generator current.

LIST OF PRINCIPAL SYMBOLS

$(\bullet)^s$	quantity (\bullet) of a synchronous particle
$(\bullet)^{\text{opt}}$	optimal values of (\bullet)
$(\bullet)_m$	maximum value of (\bullet)
J	performance index
\underline{Q}	weighting matrix for states
\underline{R}	weighting matrix for control inputs
\underline{x}	system states
\underline{k}	gain matrix
\underline{u}	control inputs
H	Hamiltonian
$\underline{\lambda}$	costates
\underline{S}	solution of matrix Riccati equation

REFERENCES

1. D. Boussard and E. Onillon, "Application of the Methods of Optimum Control Theory to the RF System of a Circular Accelerator," CERN Report SL/93-09 (RFS).
2. C.E. Kesel, M.A. Firestone, and R.W. Conn, "Linear Optimal Control of Tokamak Fusion Devices," *Fusion Technology*, Vol. 17, May 1990.
3. L.K. Mestha, C.M. Kwan, and K.S. Yeung, "Interaction Between Beam Control and RF Feedback Loops for High Q Cavities and Heavy Beam Loading," accepted for publication in the *Journal of Particle Accelerators*, LBL, Berkeley, California, USA.
4. B.D.O. Anderson and J.B. Moore, *Optimal Control: Linear Quadratic Methods*, Prentice-Hall, USA, 1990.
5. C.M. Kwan and L.K. Mestha, "Simulation of particle tracking with the inclusion of rf cavity," to be published in the *Journal of Particle Accelerators*, LBL, Berkeley, California, USA.
6. F. Lewis, *Optimal Control*, John Wiley & Sons, USA, 1986.
7. T. Kailath, *Linear Systems*, Prentice-Hall, Inc., USA, 1980.

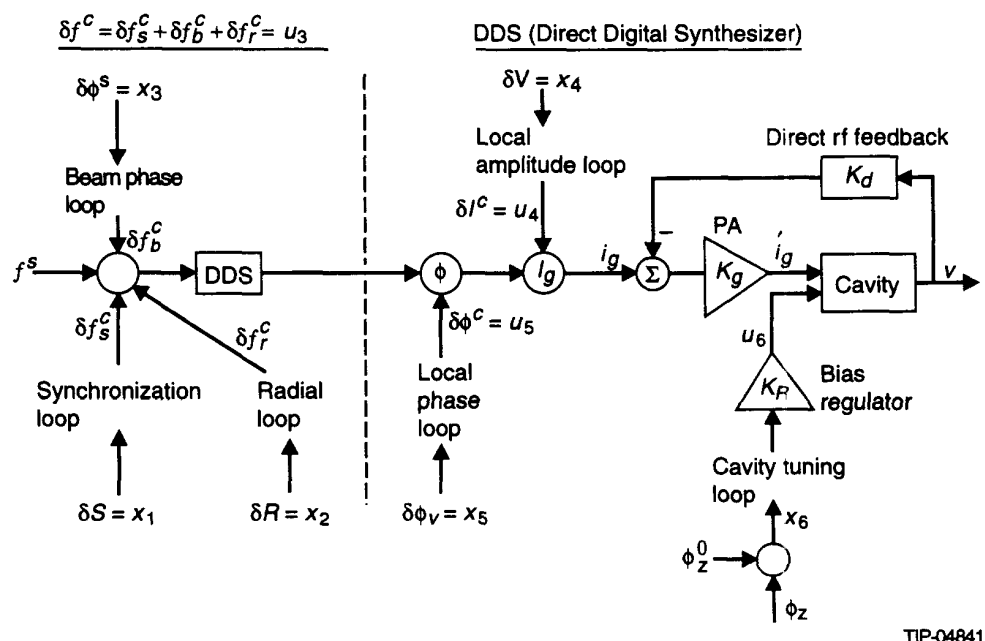
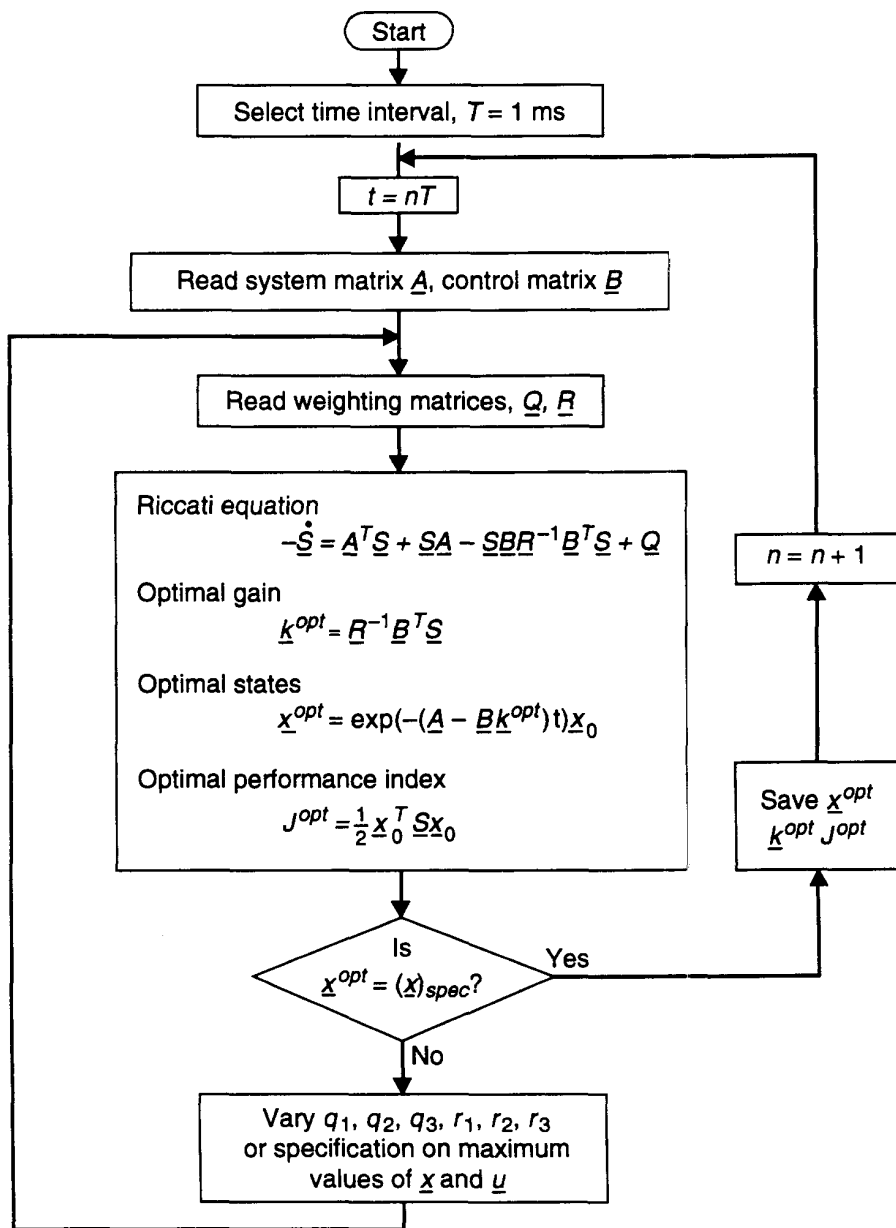
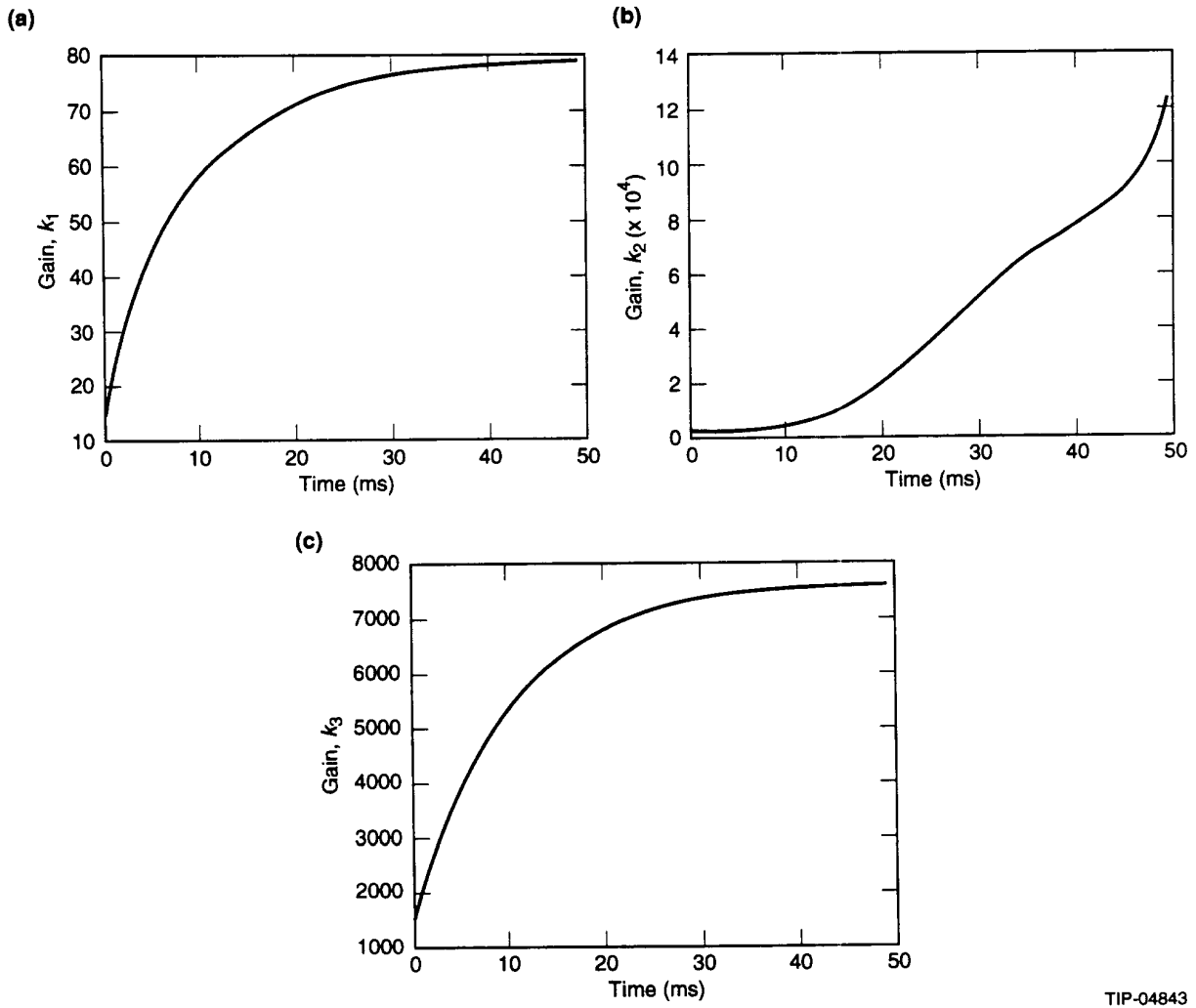


Figure 1



TIP-04842

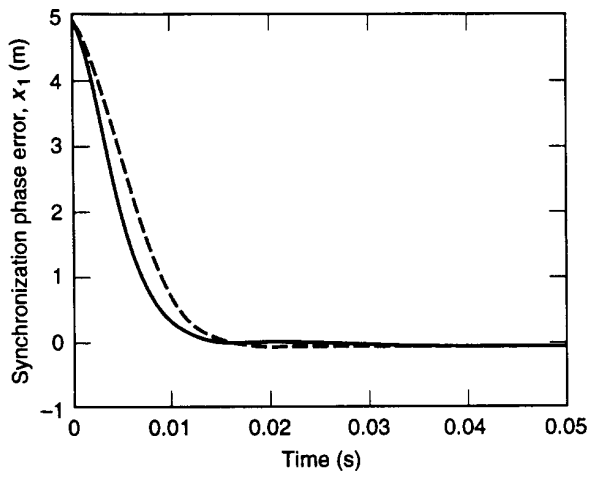
Figure 2



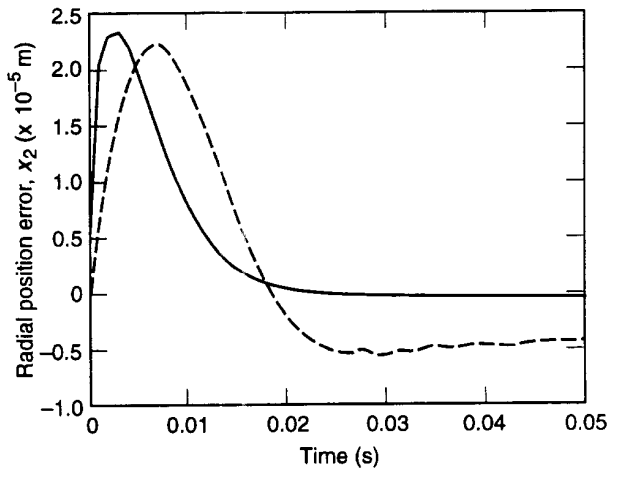
TIP-04843

Figure 3

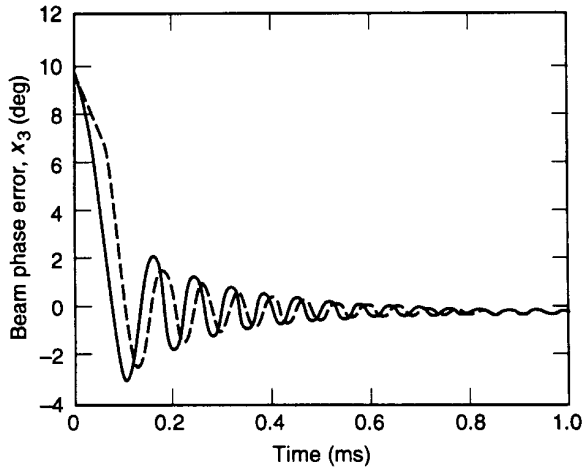
(a)



(b)



(c)



— Optimal trajectory
- - - Tracking code output

TIP-04844

Figure 4

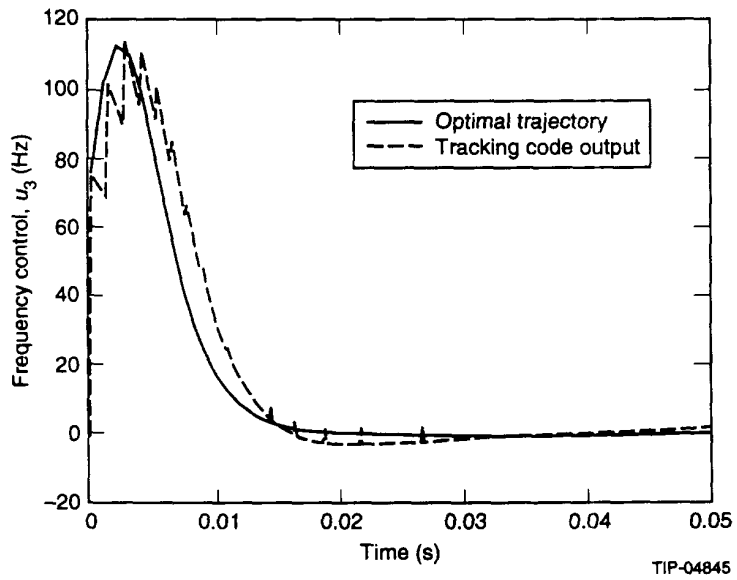
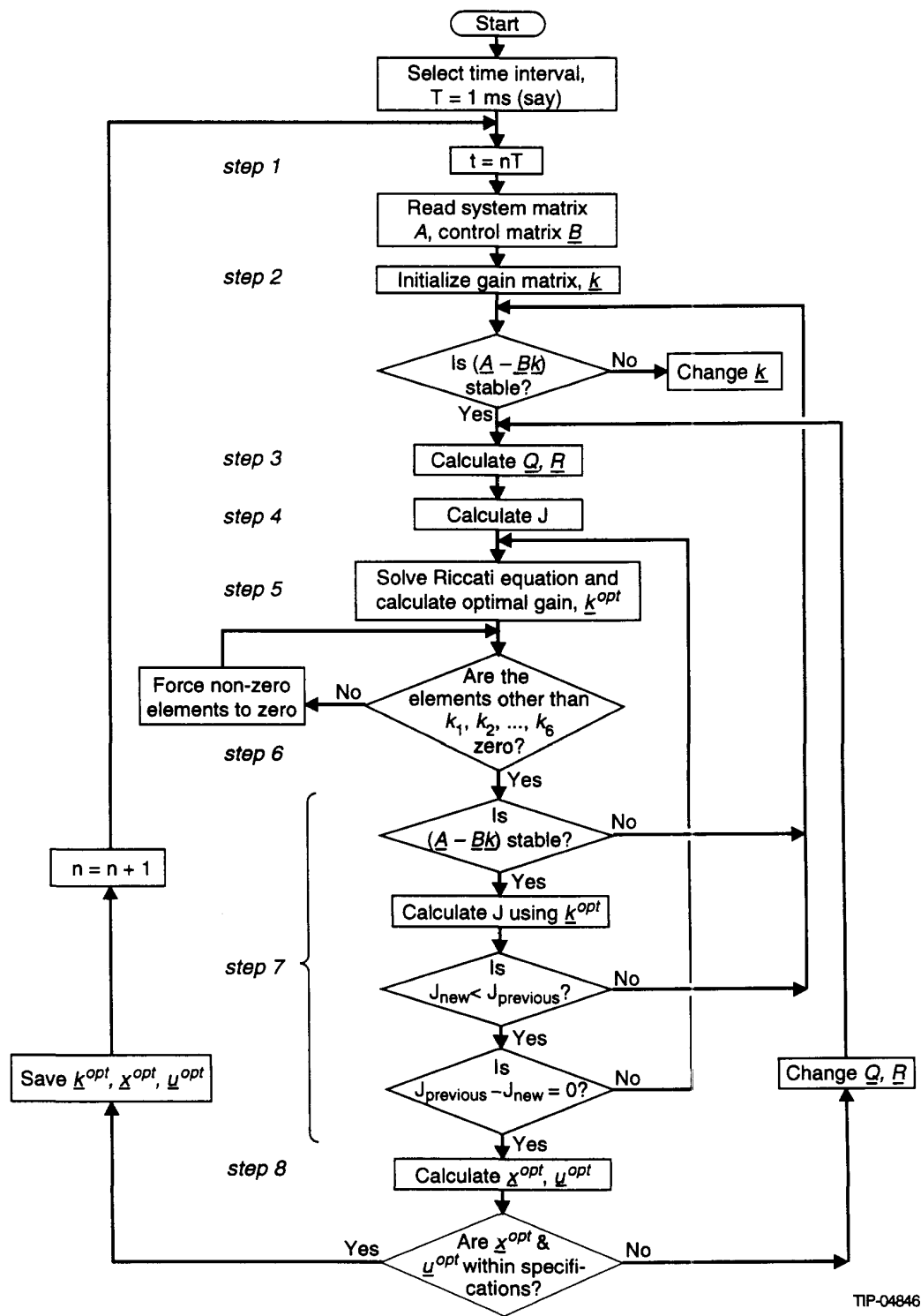


Figure 5



TIP-04846

Figure 6

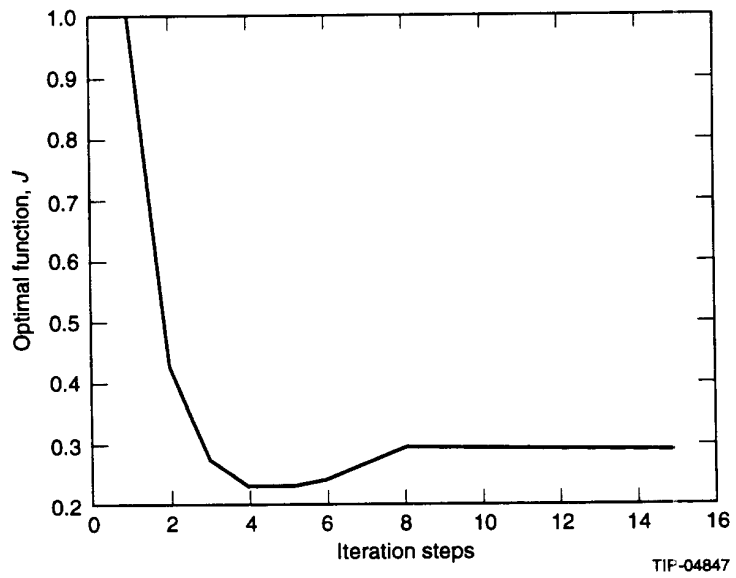
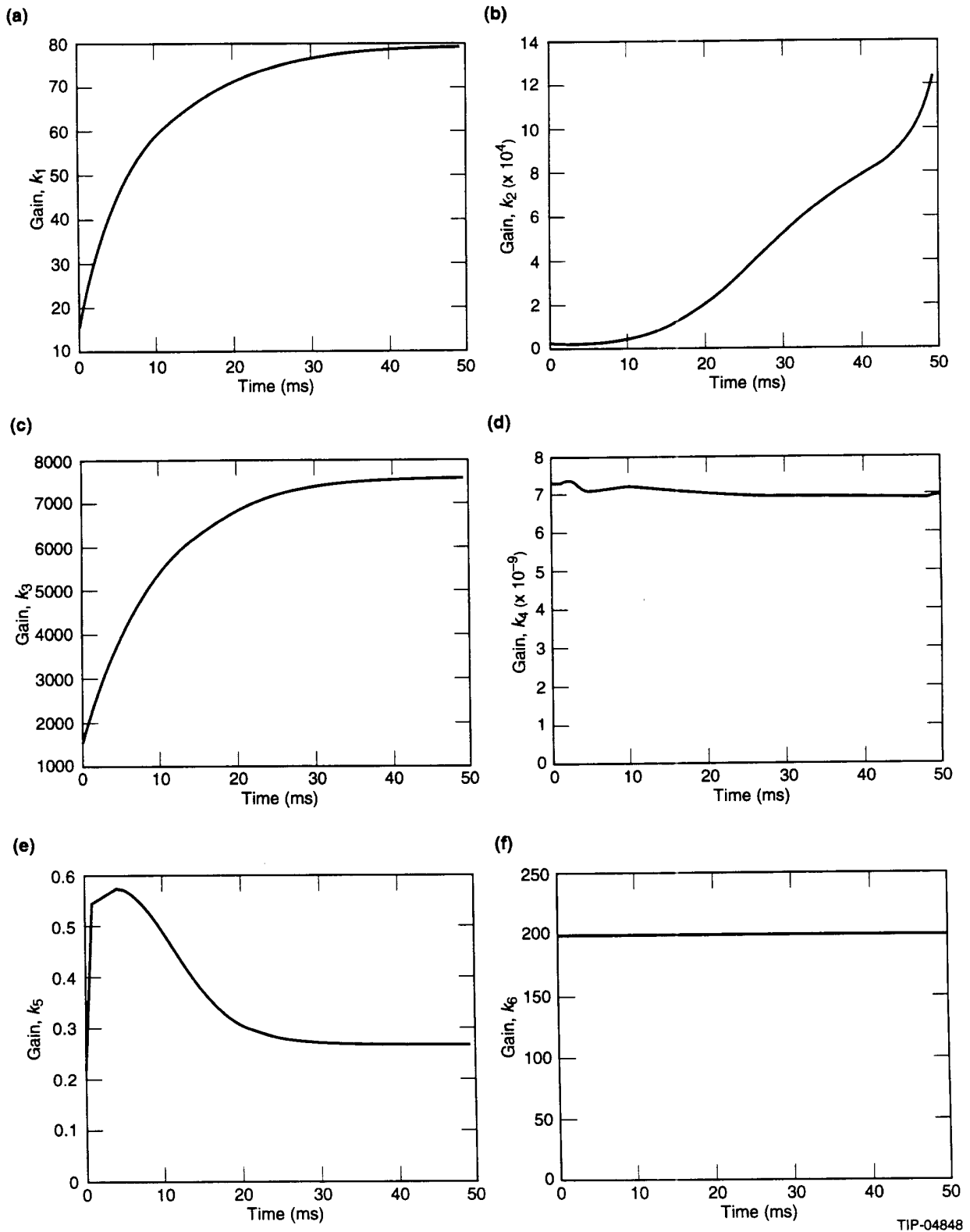
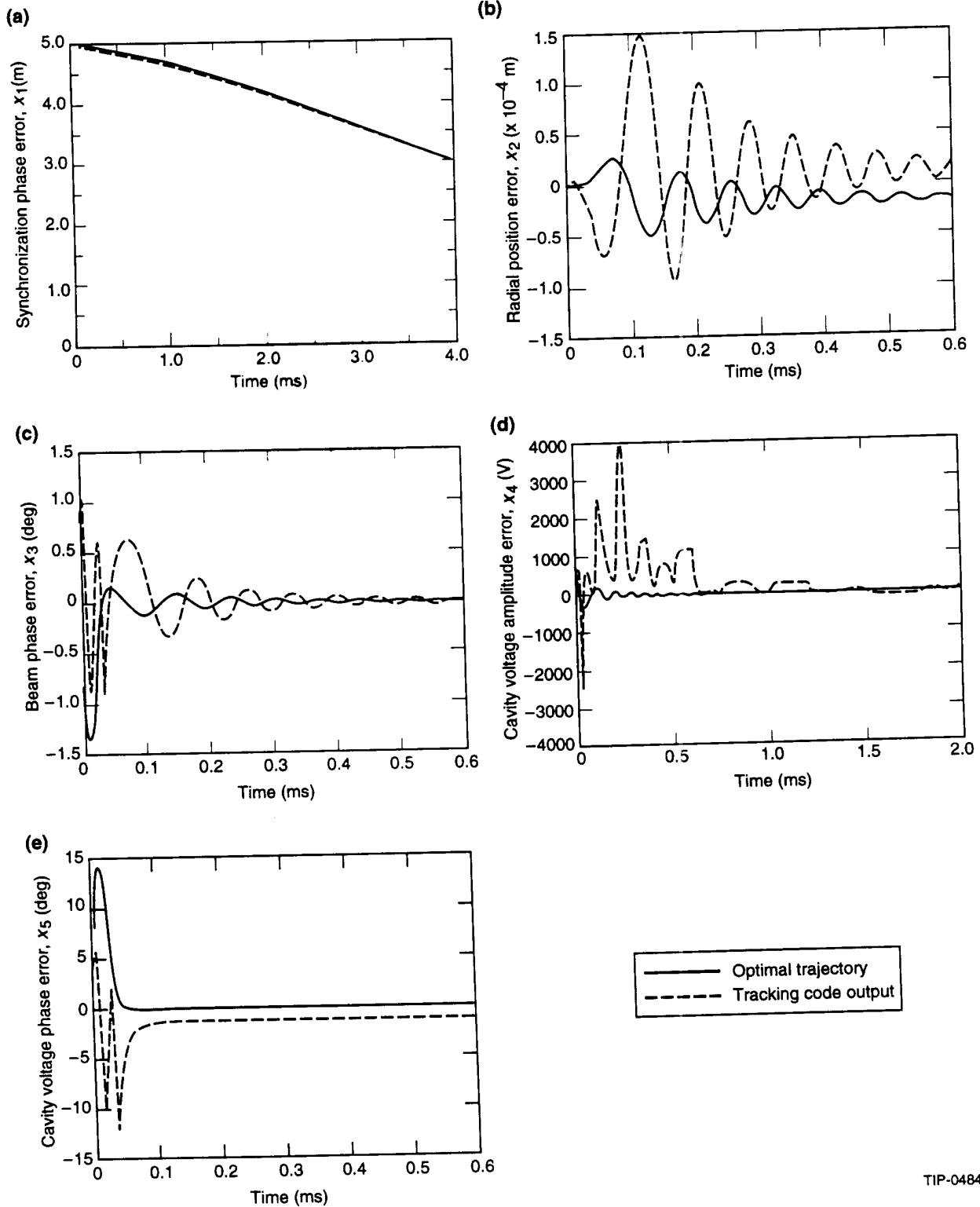


Figure 7



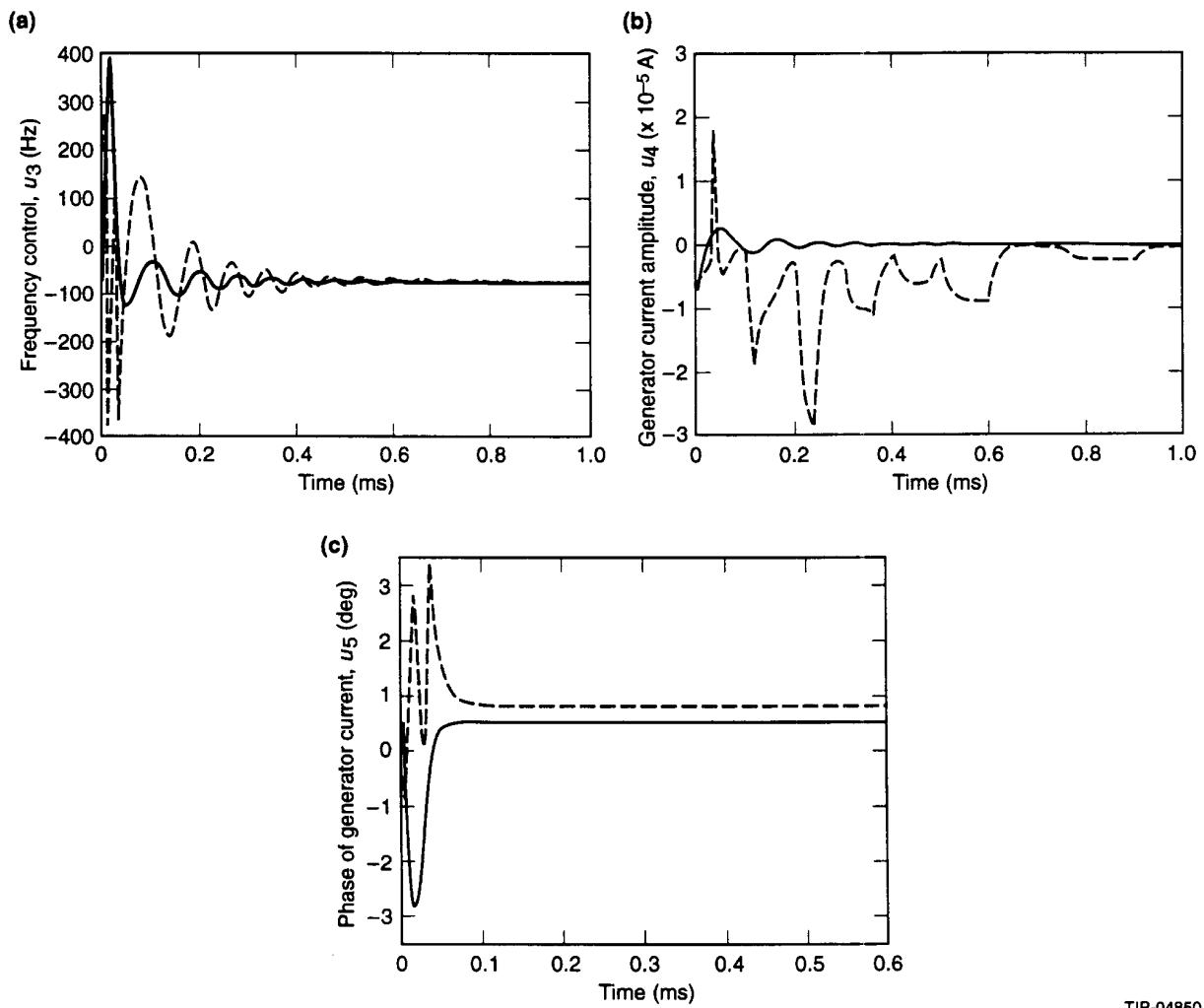
TIP-04848

Figure 8



TIP-04849

Figure 9



TIP-04850

Figure 10